4th International Symposium on Virtual Reality, Archaeology and Intelligent Cultural Heritage
VAST (2003)
D. Arnold, A. Chalmers, F. Niccolucci (Editors)

High Fidelity Lighting of Knossos

Ioannis Roussos
University of Bristol
tonsor@otenet.gr

Alan Chalmers
University of Bristol
alan@cs.bris.ac.uk

Abstract

Five kilometres from Heraklion, Crete is the Minoan Palace of Knossos. First discovered in 1878 by Minos Kalokairinos, the site today is most commonly associated with Sir Arthur Evans who bought the space in 1898 when Turkish occupation ceased in Crete. Evans excavated the site between 1900 and 1931, publishing a six volumes set "The Palace of Minos at Knossos". During his study, Evans carried out a number of "reconstructions" at the site which have been the subject of much controversy over the years. Recent developments in computer graphics enable archaeological sites to be reconstructed on a computer without any alteration of the site itself. However, if such computer reconstructions are to be meaningful tools to enable archaeologists to explore hypothesis about a site, then these reconstructions have to be high fidelity representations incorporating all known evidence including, for visualisation of the site, knowledge of the lighting that was present when the site was being used. This paper describes a high fidelity reconstruction of part of the Knossos palace including accurate modelling of flame that may have been used to light the environment in the past.

Keywords: *Physically based lighting, high fidelity graphics, virtual archaeology, Knossos.*

1. Introduction

Before the advent of electricity in the 19th century our ancestors viewed their environment by means of either sunlight or some form of flame light. As with sunlight, modern lighting appears static, flickering as it does at a rate imperceivable by the human eye. The flicker of flame light is, on the other hand, continually noticeable by the human observer, and as such may well have significantly affected the way in which an environment was perceived [2]. Furthermore, the spectral properties of flame light is very different from modern lighting which would also have had a significant effect on how, for example, colours were perceived [3]. In this paper we investigate how the lighting prevalent in ancient Crete may have affected the perception of the palace of Knossos when it was in use from 2000-1350BC.

2. Flame lighting

The study of fire and combustion falls in between physics and chemistry. To model flame accurately we need to consider both the factors which influence the flame size and stability, such airflow, and the fuel which is being burnt, which determines the colour of the light emitted.

Much previous work on modelling flame has concentrated on the propagation of large scale flames in the simulation of burning environments [9, 12, 15, 16, 17]. Recently the accurate simulation of flame has become increasingly important to the film and special effects industry [8, 11]. In this study we are interested in flames that may be categorised as diffusion wick flames, in which heat transfer from the flame cause a steady production of flammable vapour [6]. Inakage was one of the first to introduce a simplified candle flame model [7]. This was extended by Raczkowski to incorporate the dynamic nature of the flame [13].

Within this class of flame, the fuel burns as it is brought into contact with the air. On a small scale the combustion processes are then mainly determined by the rate of inter-diffusion of air and fuel. In larger flames of this type, the mixing may be due to turbulence and other movements of the gases rather than to diffusion, and in these cases the problems of flame stability and size are mostly of an aero-dynamic nature [6].

To achieve the level of fidelity we require we need to consider the different materials used for fuel, such as animal fat and beeswax, and factors which may affect the appearance of the flame, including airflow, light intensity, eye adaptation and the amount of smoke being emitted.

3. Knossos

Situated 5km from the modern Crete town of Heraklion, the Minoan Palace at Knossos covers an area of 20,000 square meters making it the largest of all the Minoan sites discovered so far. First constructed in around 2000BC, the original complex was completely destroyed

in 1700 BC by an earthquake. A second structure, which strongly resembled a labyrinth, soon replaced the destroyed earlier complex [1, 4].

In the second half of the 15th century BC a volcanic eruption from the nearby island of Thera resulted in catastrophic earthquakes, tidal waves and rains of ashes, almost destroying all life on Crete. Taking advantage of this, Achaeans from the Greek Mainland conquered the island of Crete and settled at the palace of Knossos. The palace was finally destoyed in the mid 14th century BC by a fire.

The palace had many levels and consisted of four wings arranged around a central courtyard which is oriented North-South. The east wing comprised the residential quarters including a workshop and a shrine, while the west wing contained storerooms, shrines and a throne room. On the upper floors of this wing were the banquet halls. The north wing contained the so-called "Customs House'' and the south wing the South Propylon [1, 4]. The Palace was decorated with some spectacular frescoes, many of which survived and have been restored.

We have chosen the throne room for our investigation for two reasons. First, due to its important role in ancient times. The throne room was one of the latest constructions of the palace at Knossos being constructed sometime between 1450 and 1400 BC. Although the Achaean influence is apparent in the frescos, the old Minoan religious characteristics were strong enough to be preserved or infiltrated into the new customs [1, 4]. The second reason is the painting manner of the frescos. Here is the first recorded instance of a regularized attempt to render chiaroscuro. According to Evans, the existing materials in this chamber were so full as to make possible a restoration as complete as anything of its kind. Such a type of fresco was seen again at Pompeii, a thousand and a half years later.

The throne room is entered through two doors from an antechamber. On the northern wall, off centre to the right from the entrance is the throne of Minos, made from gypsum to imitate a wooden structure, figure1.

Two wingless griffins guard it, painted on the wall one to the left and the other to the right. There are two similar griffins on the other walls of the room. These creatures, combining the strength of the lion and the vision of the sight, symbolize the royal and divine power, while wingless may symbolise their permanent presence [1]. At the back of the room, opposite the throne is a Lustral Basin. The walls are covered by lime plaster and higher up by red mortar. The throne room was illuminated by a dormer window above the basin and by stone lamps. The prevalent lighting would have had a significant impact on the impression gained of the throne room both during the day and at night.

Figure 1: The throne of Minos

4. Physically Based Lighting

For a physically accurate representation of flames, modelling only the shape is not enough, one should also take into account the light emitted from flames [3]. To provide meaningful, high fidelity simulations of the lighting within a scene physically based lighting visualisation software is required, such as Radiance [18] or 3D Studio Max ver. 5.0 which includes photometric lights and radiosity.

As mentioned above, for this study we are only concerned about modeling the illumination of candle and lamp flames. In order to have an accurate lighting model we measured the spectral data of various fuels which may have been used at Knossos including beeswax, olive oil, sesame-oil and animalfat using a spectroradiometer, figure 2. These spectral values were then converted to the CIE XYZ chromaticity coordinates and finally into RGB values which are typically used in computer graphics. Measuring spectral data of flames is not straightforward. The spectroradiometer takes several seconds to read the data at 10 nanometer wavelengths. It is important that flicker is minimised during this reading time. To reduce possible error, ten samples were taken and their average was used to compute the RGB values.

The conversion of spectrum data to RGB data that match the red, green and blue phosphors of a colour CRT, uses the tristimulus theory of colour perception, which is based on the hypothesis that our retinas have three kinds of color senses (called cones) with peak sensitivity to red, green and blue light.

The tristimulus theory is useful because it corresponds loosely to the notion that colours can be specified by positively weighted sums of red, green and blue, the so-called primary colors. A huge range of colours can be matched by positive values of RGB,

however, certain colours cannot be produced by RGB mixes and hence cannot be shown on an ordinary CRT.

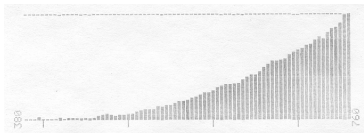

Figure 2: (a) acquiring the data with the spectroradiometer (b) burning olive-oil flame, (c) the spectral output for a beeswax flame.

Wavelengths values measured by a spectroradiometer are converted to CIE chromaticity X, Y and Z values, which characterize a standard human observer's perception of colour. The three corresponding colour matching functions $\bar{x}_l$, $\bar{y}_l$, $\bar{z}_l$ are shown in Figure 3.

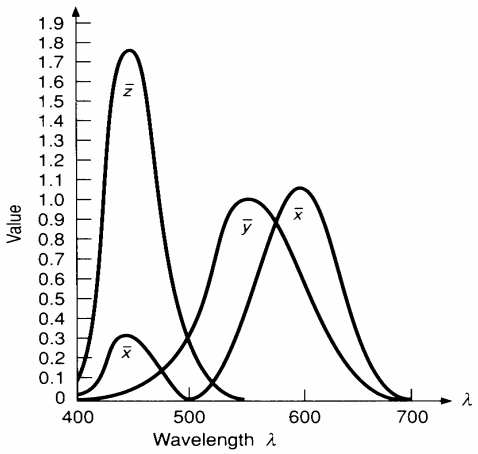

Figure 3: CIE colour matching functions

To calculate CIE X, Y and Z values we sum, over the visual range, the products of the colour matching function weights at each wavelength and the intensity emitted at a constant narrow wavelength interval, according to the following equations:

$$X = k\sum_{l1}^{l2} \bar{x}_l P(l)\Delta l$$

$$Y = k\sum_{l1}^{l2} \bar{y}_l P(l)\Delta l$$

$$Z = k\sum_{l1}^{l2} \bar{z}_l P(l)\Delta l$$

where, in each equation l_1 is wavelength at start of measurement (380 nm -violet), l_2 is wavelength at end of measurement (780 nm - red), $\bar{x}_l$, $\bar{y}_l$ and $\bar{z}_l$ are the CIE matching functions, $P(l)$ is the spectral energy and Δl is sampling interval (usually 5 or 10 nm as our measurements). Constant k is defined as

$$k = \frac{100}{\sum P_w(l)\bar{y}_l \Delta l}$$

where, $P_w(l)$ is the spectral energy for whatever light source is selected as the standard for white. For self-luminous objects like CRTs, k is usually 680 lumens/watt. For reflective objects, values are chosen such that bright white has a Y value of 100, then other Y values will be in the range of 0-100.

If **X**, **Y**, **Z** are the weights applied to the CIE primaries to match a colour **C** as found by the equations above then: C = XX + YY + ZZ

We define chromaticity coordinates, which depend only on dominant wavelength and saturation and are independent of the amount of luminous energy, by normalizing against X + Y + Z, which can be thought as the total amount of light energy.

$$x = \frac{X}{X+Y+Z}$$

$$y = \frac{Y}{X+Y+Z}$$

$$z = \frac{Z}{X+Y+Z}$$

Note that x + y + z = 1.

Finally, the chromaticity coordinates are converted to RGB using the following general equation:

$$\begin{bmatrix} X \\ Y \\ Z \end{bmatrix} = \begin{bmatrix} xr & xg & xb \\ yr & yg & yb \\ zr & zg & zb \end{bmatrix} \cdot \begin{bmatrix} R \\ G \\ B \end{bmatrix}$$

The 3x3 matrix is constructed by the chromaticity coordinates of the three phosphors of a desired CRT. Also, the chromaticity coordinates of the white that the three phosphors produce when turned on at their maximum is also needed. For our conversion, the SMPTE phosphors coordinates with a corresponding matrix was used.

Figure 4 shows a CIE chromaticity diagram. The primaries *R*, *G*, *B* define a triangle (or gamut) inside the diagram; any colour within it can be formed by mixing them. A colour may be outside the RGB primary triangle and thus will be more saturated than can be displayed; consequently it must be approximated by a less saturated colour. In Figure 4 the requested colour *C* falls outside colour gamut RGB. The line between the white point of the color system *W* and *C* includes, in the CIE diagram, all possible mixtures of *C* and *W*. The point *A* where this line intersects the RGB triangle is then the most saturated colour in the direction of *C* representable within the gamut. We use this technique to approximate out-of-gamut colors.

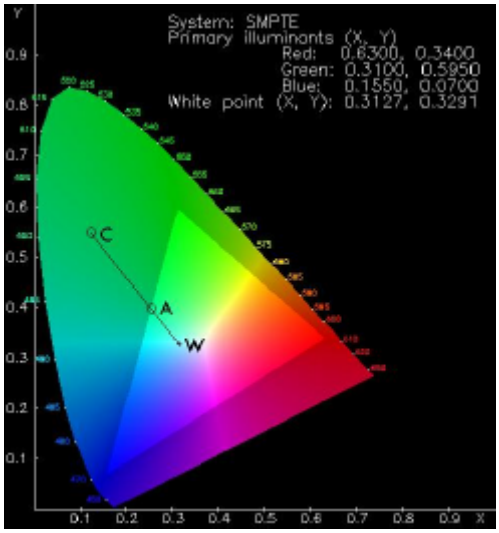

Figure 4: Requested chromaticity *C* cannot be achieved by mixing the given RGB primaries. Desaturating chromaticity *C* by mixing with the white point chromaticity *W* yields *A*, a within-gamut approximation of *C*.

4. 1 Modelling flame

As a lighting visualization system Radiance has several ways to describe a light source and supports many types of geometry and photometry data, such as the IESNA format. However, there is no equivalent photometry data or light source representation for flame lighting. Devlin and Chalmers represented their flame as a series of Radiance *illum* spheres which approximated the shape of a flame acquired from a video sequence [3]. The goal for our work was to create an arbitrary flickering flame (which could later be related to actual airflow within the environment) that was not only an accurate approximation of a real flame, but also efficient to compute. The important question was how to best to represent the geomety of an arbitrary flickering flame and thus its illumination at each time step.

Light emitted by flame sources is isotropic. To simulate this type of light our first approach was to create a bounding volume of smaller voxels (cubes of size one) that encompassed the entire flame. As the flame flickered, we could turn on or off each individual cube that was occupied by the flame. Then, only voxels turned on would contribute to the overall illumination. To confirm our theory, we tested it with a simple box light source. An image with that light source was rendered. Then, this cube was divided into equal parts. For each smaller light source part, a new image was rendered. Our theory would be correct if the sum of partial light sources would contribute the same amount of light as the whole light source in the original image. Indeed, the following equation was true

$$I_{RGB} = \sum_{i=1}^{i=n} I(i)_{RGB}$$

where, I_{RGB} is the original image (rendered by the source light as a whole), i is the number of light sources (therefore the number of images), $I(i)_{RGB}$ is each image.

However, for a flame, some voxels of the bounding volume would never be occupied by the flame even when it flickered to its extremes. Moreover, only a portion of the voxels would ever fully be fully occupied by the flame. To optimise our model of the overall illumination we needed to determine the percentage contribution of each voxel.

A first optimization was to approximate the volume in which the flame resides by a sphere and place it in the center of the flame, then by the equation of a sphere in 3D space:

$$(x-x_0)^2+(y-y_0)^2+(z-z_0)^2=r^2$$

it is very easy to determine which voxel is inside or outside the sphere and therefore if that particular voxel contributes to the flame illumination. If the distance of the center of the box and the center of the sphere is greater than the radius of the sphere, we know that this voxel is not part of the total illumination.

Our original bounding volume, the cube, consisted of 1000 smaller light voxels and the rendering time for a very simple test scene, Figure 6, was three and a half hours on a P4 2.4GHz processor. The spherical bounding volume optimization comprised less than 880 light cubes and the rendering time for the same scene and processor, was reduced to three hours. Most importantly, however, both methods suffered from serious artifacts such as unnatural shadows and illumination, as it is evident in figure Figure 6.

In an attempt to overcome these problems, the volume of light cubes was substituted by a single sphere of the same size. Perhaps not surprisingly, the artefacts were removed, but more importantly, there is close match of the resultant image to the real flame and the dramatic reduction in the rendering time to less than 30 seconds. This simple light sphere was also suitable for arbitrarily flickering flames.

Figure 6: Bounding volume cube as flame light source, artifacts are more than obvious

4.2 Validation

A real reference scene, containing various geometrical objects was constructed and was compared to our computer reconstruction of this test environment. The objects were of different sizes and placed in a particular way in the scene in order to test and evaluate our model in various scenarios. At a later stage, concentric circles were added at the base of the “floor”, to make more accurate measurements and observations. Burning candles in the real scene, under normal burning conditions, were captured using video and photographs, in a completely dark room. Then, an image was rendered in Radiance with the same setup and a view close to that of the photograph. This synthesized image then was compared to the real scene and the photographs and video. Of interest were the visual characteristics of candle flame including the shadows, the illumination, and of the flame. Figure 7 shows a photograph of the real scene and its virtual reconstruction. The measurements made in this validation step were used to improve the fidelity of the virtual flame which was then used in our Knossos reconstruction.

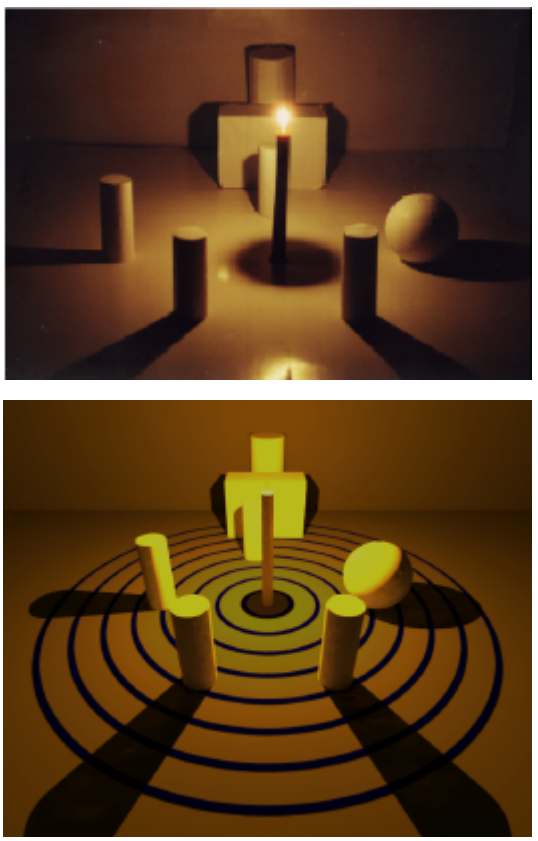

Figure 7: Test environment (a) Photograph of real scene (b) virtual reconstruction

5. Virtual Knossos

The throne room was modelled in 3D Studio. Information regarding dimensions of the room, throne, columns etc, and materials, frescos, painting colours etc. were collected from [4]. The model consists of 137,456 polygons. The scene was rendered using three different light scenarios, modern lighting, beeswax candle and daylight. Lights in the scene were positioned to illuminate the area of interest, the middle of the room, that is, between the throne and the lustral basin. This choice of position of the modern and candle lighting was quite arbitrary. Our system can allow archaeologists to explore where the lighting might have been best placed to provide appropriate lighting within the environment while not interfering with the use of the site.

Figure 8 shows the wireframe model for the throne room, figure 9 the throne room lit by a beeswax candle and figure 10 the same view lit by a modern electric light of two 32-watt fluorescent lamps. Finally figure 11 shows the throne room in daylight as may have been present at noon on 18 August 1400 BC.

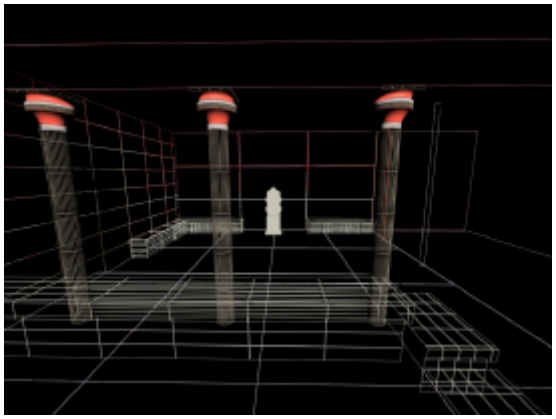

Figure 8: Wire fame model

Figure 9: Throne room lit by beeswax candle

Figure 10: Site lit with modern electricity

Figure 11: Noon, 18 August 1400 BC

6. Conclusions

We have presented an efficient, physically based model of small flame lighting, such as candles of different materials. This model is suitable for both static images and one with a flickering flame. This model has been used to produce a high fidelity reconstruction of the throne room in Knossos. As the images clearly show, there is a significant perceptual difference from a reconstruction of this site lit by modern electric lighting models prevalent in most computer modelling packages, and the high fidelity physically based illumination of candle light. Future work will investigate this perceptual difference in more detail using, for example, Myszkowski's Visual Difference Predictor [10].

To provide a useful tool to archaeologists, it is important to provide such high fidelity images in real time to enable them to investigate hypotheses of site lighting interactively. Future work will investigate the creation of dynamic light-maps of our spherical light sources based on physical properties of airflow such as velocity and direction. The light maps will then be applied onto pre-

rendered images to simulate the behaviour of flickering flames lighting, in real-time. In addition, the key issue of colour adaptation will need to be addressed in the future to ensure the highest fidelity of our resultant images. We will also investigate whether full spectral rendering, as opposed to just RGB, will make a significant difference in the perception of reconstructed heritage environments.

Acknowledgements

We are grateful to the Alexander S. Onassis public benefit foundation for providing the funding for Ioannis to undertake this research.

References

1. Alexiou S., *Minoan Culture*, 6th Edition, Alexiou & Sons Publications, Crete
2. Chalmers A., Green C. and Hall M., *Firelight: Graphics and Archaeology*, Electronic Theatre, SIGGRAPH 00, New Orleans, 2000.
3. Devlin K. and Chalmers A., *Realistic visualisation of the Pompeii frescoes*, Proceedings of AFRIGRAPH 2001, 2001.
4. Evans A.J., *The palace of Minos at Knossos*, vol IV, London, 1934
5. Gardner G.Y., *Modeling Amorphous Natural Features*, in *SIGGRAPH 94 Course 22*, 1994.
6. Gaydon A.G. and Wolfard, H.G,, *Flames: Their Structure, Radiation and Temperature*. Chapman and Hall, 1979
7. Inakage M., *A simple model of flames*, Proceedings of Computer Graphics International, Springer-Verlag, pp. 71-81, 1990.
8. Lamorlette A. and Foster N., *Structural modelling of natural flames*, Proceedings of SIGGRAPH 2002, ACM SIGGRAPH, 2002.
9. Mavrodineanu R. et al., *Analytical Flame Spectroscopy, Selected Topics*. (1970) MacMillan.
10. Myszkowski K., Tawara T., Akamine H. and seidel H-P., *Perception-Guided Global Illumination Solution for Animation Rendering*. In Proceedings of SIGGRAPH 2001, pp. 221-230, ACM SIGGRAPH, 2001.
11. Nguyen D., Fedkiw R.P., Jensen W., *Physically based modelling and animation of fire*, Proceedings of SIGGRAPH 2002.
12. Devlin K., Chalmers A., Wilkie A., and Purgathofer W., *STAR: Tone Reproduction and Physically Based Spectral Rendering*, State of the Art Reports, Eurographics 2002, pp. 101-123. The Eurographics Association, 2002
13. Raczkowski J., *Visual Simulation and Animation of a laminar Candle Flame.* International Conference on Image Processing and Computer Graphics, Poland, 1996.
14. Reeves W.T., *Particle Systems - A Technique for Modeling a Class of Fuzzy Objects*. *Proceedings of ACM SIGGRAPH 83*, pp. 359-376, 1983.
15. Rushmeier, Holly E., *Rendering Participating Media: Problems and Solutions from Application Areas.* Proceedings of the Fifth Eurographics Workshop on Rendering, Springer-Verlag, 1995.
16. Sakas G., *Cloud modeling for visual simulators*, in G. von Bally and H.I. Bjelkhagen, editors, *Optics for protection of man and environment against natural and technological disasters* Elsevier Science Publishers B.V., pp.323-333, 1993.
17. Stam J., Fiume E., *Turbulent Wind Fields for Gaseous Phenomena*. Proceedings of SIGGRAPH 93, pp.369-376, 1993.
18. Ward Larson, G. and Shakespeare, R., *Rendering with RADIANCE: The art and science of lighting simulation*. Morgan Kauffman, 1998.